Characterization of Novel Lightweight Radiation Shielding Materials for Space Applications

Michael Steffens, Felicitas Hepp, Stefan K. Höffgen, Phillip Krzikalla, Stefan Metzger, Frank Pellowski, Giovanni Santin, Lars Tiedemann, Adrian Tighe, Udo Weinand

Abstract—**Novel materials or multilayers can help to reduce the mass requirement for radiation shielding of electronic components significantly. In this study, potential alternatives to the standard aluminum shielding approach are assessed by Monte Carlo simulations and promising candidates are manufactured and characterized by radiation tests including proton and electron tests. The transmission of energetic protons of up to 39 MeV through the shielding solution was assessed as well as the dose deposited by energetic electrons up to 12 MeV in RADFETs and Alanine dosimeters behind the shield.**

I. Introduction

PRESENTLY, the shielding of electronic components from high energy radiation in space is relying on a) the shielding provided by the surrounding spacecraft structure and adjacent systems, b) the shielding capacity of aluminum electronic housings with sufficient wall thickness and c), if feasible, the implementation of spot shielding at component level. This standard approach is challenged e.g. by the need to utilize commercial instead of rad-hard electronic parts, by missions in extreme environments (e.g. the JUICE Jupiter mission [1]) or by longer exposure to Earth's radiation belts (e.g. by an extended geostationary transfer orbit (GTO) phase when electrical propulsion systems are used [5]). In any of these cases the standard approach would lead to an overall increasing shielding mass due to e.g. excessively thick housings.

Novel materials and material combinations can simultaneously help to reduce the mass requirements and also to increase the overall shielding performance. This study will investigate promising shielding solutions where the shielding will not only depend on the overall applied mass but will also make use of the physical effects involved, especially by assessing combinations of High- and Low-Z materials or compounds thereof. These new materials will be evaluated upon their suitability as a more efficient radiation protection material including some crucial tests necessary for space qualification. This study will focus on the shielding properties of bare material slabs against ionizing radiation.

This work is supported by the European Space Agency under contract number 4000111470/14/NL/RA.

Lars Tiedemann, Felicitas Hepp and Philipp Krzikalla are with HPS GmbH, München (e-mail: tiedemann@hps-gmbh.com, hepp@hps-gmbh.com, Krzikalla@hps-gmbh.de).

Stefan K. Höffgen, Stefan Metzger, and Michael Steffens and Udo Weinand are with Fraunhofer INT, 53879 Euskirchen, Germany (e-mail: stefan.hoeffgen@int.fraunhofer.de, stefan.metzger@int.fraunhofer.de, michael.steffens@int.fraunhofer.de, udo.weinand@int.fraunhofer.de).

Frank Pellowski is with OHB-System AG (e-mail: frank.pellowski@ohb.de).

Giovanni Santin and Adrian Tighe are with ESA-ESTEC (e-mail: Giovanni.santin@esa.int, Adrian.tighe@esa.int)

II. Material Selection and Trade-off Analysis

Material selection started from a vast initial list of potential materials and material combinations. These were analyzed with respect to their shielding properties by Monte Carlo simulations and with respect to market availability, machinability and bonding of the different materials.

For the first analysis, several mission scenarios of high commercial or scientific interest like e.g. a standard LEO mission or the upcoming JUICE mission [1] were considered and the environmental shielding performance was analyzed using MULASSIS [2] on the SPENVIS [3] platform. Some simulation results of a GEO mission with extended GTO phase are shown in Fig. 1.

This was one input into a trade-off where relevant material properties, producability and machinability, as well as commercial feasibility and sustainabilitywere contributing factors.

This reduced the initial list of materials to four shielding solutions which includes multilayer stacks of High- and Low-Z materials as well as homogeneous compounds of High- and Low-Z materials. While we currently cannot disclose the exact composition and processing of the materials, the solutions making the final list of materials are Ta-enhanced carbon-fiber-reinforced-plastic (CFRP) (Material A), W-enhanced polyethylene (PE) (Material B), W-enhanced polyamide (PA) (Material C) and epoxy enhanced with High-Z-additives (Material D).

III. Sample Preparation

Samples for measuring the proton and electron shielding performance of the material consist of slabs of approximately $20 \times 20\ cm^2$ size. The samples for the four selected shielding materials were manufactured and processed by specialized

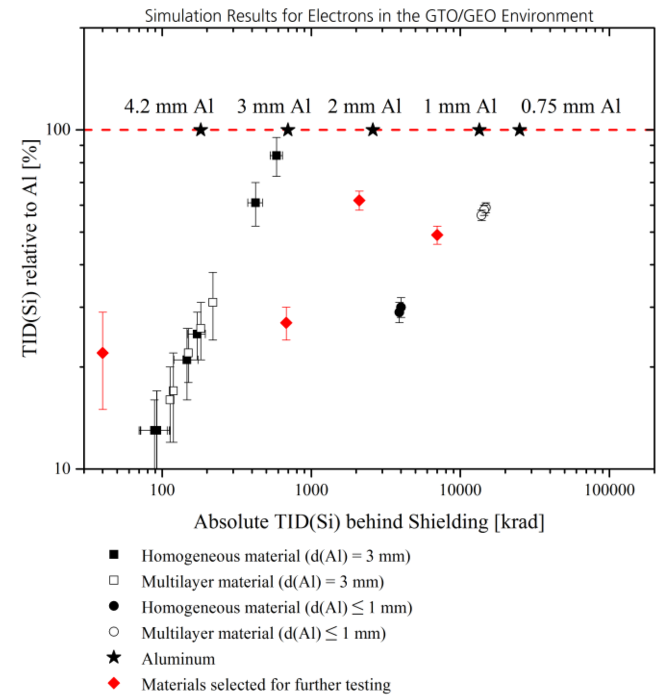

Fig. 1. Simulation results of various shielding solutions in an electron environment for a hypothetical GEO mission with extended GTO phase. Materials are grouped by type (multilayers and homogeneous) and by thickness. The materials which passed the full trade-off analysis are highlighted in red.

suppliers and manufacturers. The thickness of the Al99.5 reference samples is tailored to give the same mass per area for each individual shielding material for a consistent comparison to the equivalent aluminum shielding measurement. Aluminum foils were added when matching slab thicknesses were not available.

IV. Radiation Test Procedures and Setups

This contribution will focus on the results of the radiation shielding tests. A range of standard materials tests (e.g. outgassing, thermal cycling, mechanical strength, lap shear) were performed, some after radiation ageing of the samples with Co60, to assess the overall potential for use of the materials for space applications.

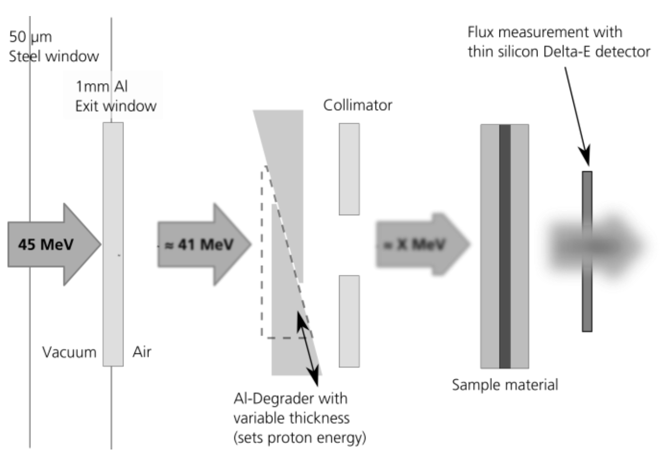

Fig. 2. Test setup for proton transmission measurement. The proton flux is evaluated behind the sample material. The proton energy is tuned by an Al-degrader of variable thickness. In the photograph the setup is shown from the back with the parts of the accelerator grayed out.

Proton testing took place at the JULIC cyclotron at FZ Jülich, which provides protons with initial energy of 45 MeV. Taking the exit windows of the beam line and a short path through ambient air into account, the energy at the test setup is approx. 41 MeV. Using an additional Al-degrader of variable thickness (see Fig. 2), the proton mean energy can be further reduced. As a side effect, the energy distribution will also be broadened, which limits the applicable degrader thickness to be less than 7.75 mm.

The degrader consists of two equally dimensioned wedges, with one of them attached to a step motor. Each 1 mm shift of that wedge leads to a thickness variation of 50 µm of the degrader. Transmission will occur when the protons have sufficient energy to pass the degrader and the material with some kinetic energy left and the ionization by the protons can be detected in a Si- detector behind the sample.

Radiation shielding tests with electrons took place at the "Elekta Precise Treatment System" clinical electron accelerator at the Physikalisch-Technische Bundesanstalt (PTB) Braunschweig with electron energies between 4 and 22 MeV and additional tests with an energy of 1.5 MeV at the ELV-2 facility at the Leibniz-Institute für Polymerforschung (IPF), Dresden with access provided by Fraunhofer FEP, Dresden.

In the tests we measured the total dose behind the shielding material or mass-equivalent aluminum both with alanine pellet dosimeters, which can be traced to international dosimetry standards, and for immediate readout also with RADFETs (Fig. 3). The data from RADFETs and the alanine behind shielding are scaled to an arbitrary value of 10 Gy with respect to the dose level of the upper alanine pellet to account the different dose levels from run to run and at the two facilities.

At the ELV-2 facility, the stack of the shielding materials with top and bottom alanine pellets and the RADFET readout board, with all pins of the devices shorted, were transported by a conveyer to the irradiation area. The dose deposited during the transport through the extent electron beam is set by the transport velocity. The alanine results indicate dose levels of around 500 Gy per run above the shielding. The RADFET readout was performed once after irradiation of each sample.

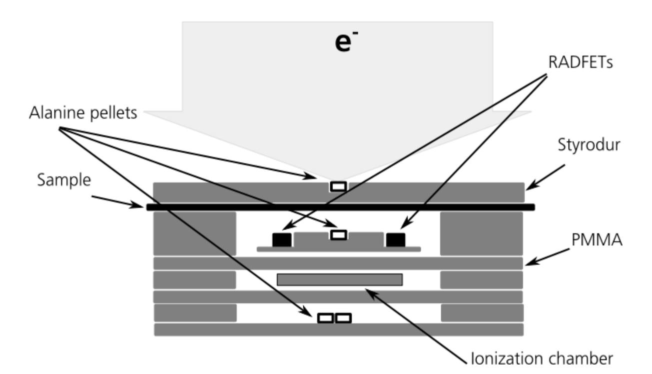

Fig. 3. Test setup at PTB for measurement of total dose by electrons behind shielding with alanine dosimeters and four RADFETs.

During data evaluation, the dose detected by the RADFETs and the bottom alanine was again scaled to a nominal dose of 10 Gy based on the results of the top alanine pellet. For both campaigns the alanine readout was performed at PTB, Braunschweig. To achieve sufficient accuracy over the range of observed doses, the readout system at PTB was calibrated by additional Co-60 irradiation of alanine dosimeters.

V. Results

The results of the proton transmission measurements for the four shielding solutions is shown in Fig. 4 with closed symbols indicating the novel shielding materials and open symbols indicating the respective mass-equivalent aluminum. Of the materials considered in these tests, only W-enhanced PE (Material B) is performing slightly better than aluminum when exposed to protons. Protons up to 12.5 MeV are fully stopped in the shielding material. This was already anticipated in MULASSIS simulations on the SPENVIS platform [3] performed prior to testing.

There is however a constant slope in the data, with transmission increasing from low energies (large degrader thickness) to high energies (low degrader thickness) depends on the increased scattering of the protons away from the collimator axis with the degrader thickness.

Results for the shielding tests with electrons of both campaigns are shown in Fig. 5. Closed symbols indicate the total dose as given by the alanine measurements open symbols the total dose in the RADFETs for both the samples and the respective mass-equivalent aluminum. Error bars indicate the 1-sigma standard deviation of the four RADFETs.

As was mentioned above these data were scaled with respect to the dose deposited in the top alanine pellet. The dashed lines represent MULASSIS simulations of the

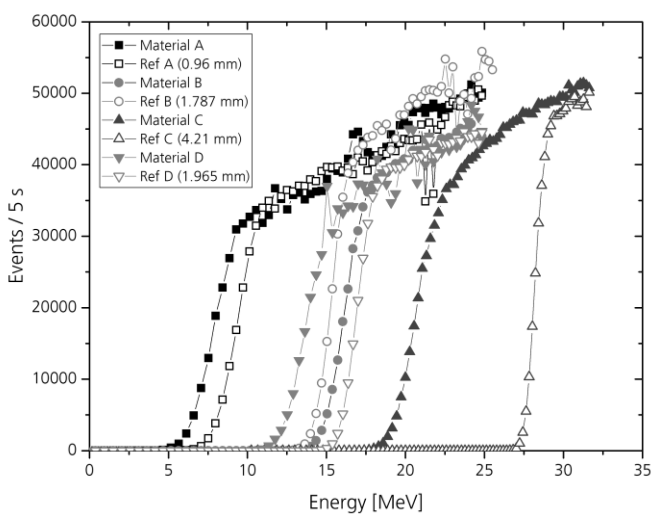

Fig. 4. Proton transmission measurements for materials A-D (full symbols) and corresponding aluminum slabs (open symbols). Starting from some minimum energy, protons start passing through the sample. The higher that threshold energy is, the better the shielding for protons. If the corresponding aluminum transmits protons at lower energies, then the shielding performance of the material is better than aluminum. In these measurements, this is only the case for W-enhanced polyethylene (PE) (Material B).

RADFET geometry. It should be noted that the results obtained in these simulations are doses per 10^{10} electrons, so the scales of the y-axis are set more or less arbitrary but identical in all four plots. A relatively good match between the simulated curve and the alanine data can be seen, there are however some discrepancies in the RADFET data. As the threshold electron energy for dose deposition is in any case higher for the sample materials than for the mass-equivalent aluminum, each of the solutions has superior shielding properties compared to the respective mass-equivalent aluminum. Only materials A and B transmit electrons of 1.5

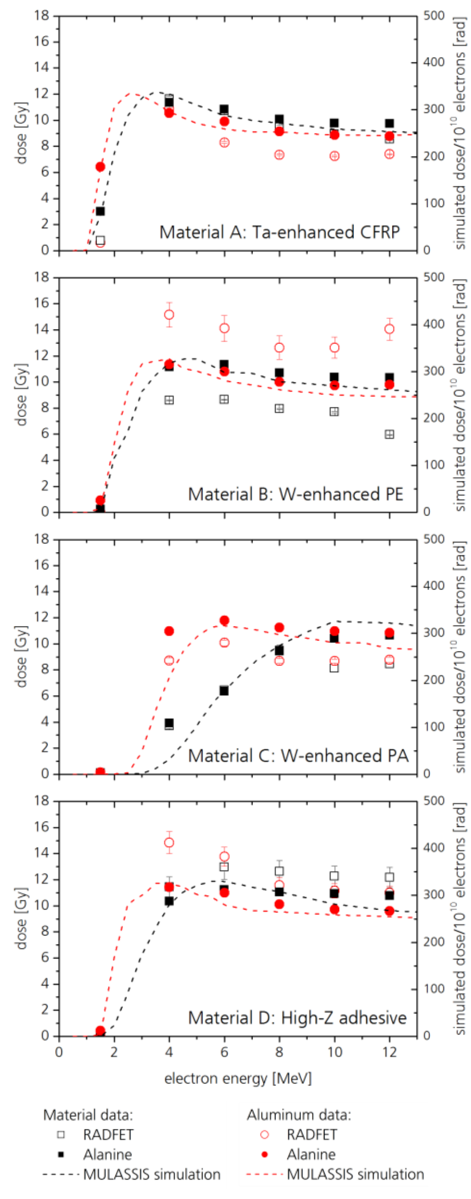

Fig. 5 Results of total dose measured in RADFET and alanine dosimeter behind shielding when exposed to electrons. Similar to proton flux measurements, the higher the electron energy required for radiation to deposit significant amounts of dose, the better the shielding properties. When comparing the results to MULASSIS simulations, there is a good match with alanine data but large discrepancies to the RADFET data. Each material tested has however superior shielding properties compared to mass-equivalent aluminum. This is most pronounced for Material C and least for Material A.

MeV energy, the results for C and D are comparably negligible.

VI. Conclusion

W-enhanced PE (Material B) may be best suited for proton dominated environments. As this material provides some structural stability, it may be well suited for electronic housings or at least for an additional lining of an electronic housing. This material did however did not pass some mechanical tests after thermal treatment, so the chance of a working implementation may be limited.

W-enhanced polyamide (Material C) is especially suited for environments where the total dose is dominated by the electron contribution. It does not provide structural stability. Being electrically insulating, the obvious implementation would be as a spot shield.

Acknowledgements

We would like to thank the staff of the irradiation facilities, especially Dr. Ralf Gebel and Dr. Olaf Felden (IKP, FZ Jülich), Dr. Ralf-Peter Kapsch (PTB) and Javier Portillo (Fraunhofer FEP) for their support in conduction the radiation campaigns. We also would lke to thank Thomas Hackel (PTB) for alanine evaluation.

References

[1] O. Grasset, M. K. Dougherty, A. Coustenis, E. J. Bunce, C. Erd, D. Titov, M. Blanc, A. Coates, P. Drossart, L. N. Fletcher, H. Hussmann, R. Jaumann, N. Krupp, J.-P. Lebreton, O. Prieto-Ballesteros, P. Tortora, F. Tosi, and T. van Hoolst, "JUpiter ICy moons Explorer (JUICE): An ESA mission to orbit Ganymede and to characterise the Jupiter system," *Planetary and Space Science*, vol. 78, pp. 1–21, 2013.

[2] F. Lei, P. R. Truscott, C. S. Dyer, B. Quaghebeur, D. Heynderickx, P. Nieminen, H. Evans, and E. Daly, "MULASSIS: a Geant4-based multilayered shielding simulation tool," *Nuclear Science, IEEE Transactions on*, vol. 49, no. 6, pp. 2788–2793, 2002.

[3] D. Heynderickx, B. Quaghebeur, J. Wera, Daly, E. J, and Evans, H. D. R, "New radiation environment and effects models in the European Space Agency's Space Environment Information System (SPENVIS)," *Space Weather*, vol. 2, no. 10, pp. S10S03, 2004.

[4] ESA-ESTEC (TEC-EES & SRE-PAP), „JUICE Environmental Specification," JS-14-09, issue 5, revision 3, 17.10.2014

[5] J. G. del Amo (2015, July), "European Space Agency (ESA) Electric Propulsion Activities". Presented at Joint Conference of 30th International Symposium on Space Technology and Science 34th International Electric Propulsion Conference and 6th Nano-satellite Symposium,. [Online]. Available: http://epic-src.eu/wp-content/uploads/2015-b-IEPC-02.pdf (Last checked on 2016-04-13)